

Strain Effects on Physical Gelation of Crystallizing Isotactic Polypropylene

NATALIA V. POGODINA,¹ H. HENNING WINTER,¹ SRIVATSAN SRINIVAS²

¹ Department of Polymer Science and Engineering, and Department of Chemical Engineering, University of Massachusetts at Amherst, Amherst, Massachusetts 01003

² Exxon Chemical, 5200 Bayway Drive, Baytown, Texas 77522

Received 28 April 1999; revised 5 August 1999; accepted 5 August 1999

ABSTRACT: Early stages of crystallization of polymers may be viewed as thermoreversible physical gelation in which molecular connectivity is introduced by crystallization. Effects of shear strain on the early stages of crystallization of a commercial isotactic polypropylene are studied by dynamic mechanical experiments. Shear creep with large strains (up to $\gamma = 300$) on the undercooled melt for short times (the time did not exceed 100 s) was followed by small amplitude oscillatory shear (SAOS) at a strain amplitude ($\gamma_a = 0.01$) for gel-point detection. The imposed shear strongly accelerates gelation; gel times decrease in a power law with increasing strain. Strain applied during the crystal growth stage enhances gelation much stronger than strain applied in the earlier nucleation stage. For rapid gelation, frequency sweeps are not possible and new methods for gel-point detection need to be explored; here, we propose to estimate the gel point from the storage modulus growth at a single frequency. A value of 10% of the total growth of G' was found to be a good estimate for the gel point. High strain experiments show the complexity of underlying mechanisms of strain-enhanced crystallization and reveal at least two sequential stages in the structure development under shear: at the first stage, crystalline regions connect molecules into a loose network; at the second, stage-intense crystallinity growth within the network proceeds. Results have industrial importance in predicting/tuning structure development and connectivity growth during nonisothermal processing. Morphological study of the early stages of crystallization under strain is underway to explore molecular mechanisms, which govern the gelation process. © 1999 John Wiley & Sons, Inc. *J Polym Sci B: Polym Phys* 37: 3512–3519, 1999

Keywords: shear; crystallization; gel point; polypropylene

INTRODUCTION

The dynamics of crystallization has been extensively studied during the past decade using a variety of techniques including microscopy, SALS, SAXS and WAXD, DSC, FTIR, rheology,

and so forth, and are summarized in excellent reviews.^{1–4} Crystallization in polymers occurs through a nucleation and growth mechanism. When clusters are growing, molecular mobility slows down. Distances over which molecular motions are correlated (correlation lengths) are increasing. At the critical gel point (GP), growing clusters impinge and the correlation length diverges to infinity. At this instant, an interconnected network arises and the system undergoes liquid–solid transition. Thus, a crystallizing polymer may be viewed as a thermoreversible gel in which molecular connectivity is introduced by

Dedicated to Professor H. G. Fritz, Stuttgart, Germany, on the occasion of his 60th birthday

Correspondence to: H. Winter (E-mail: winter@acad.umass.edu)

Journal of Polymer Science: Part B: Polymer Physics, Vol. 37, 3512–3519 (1999)
© 1999 John Wiley & Sons, Inc. CCC 0887-6266/99/243512-08

crystallization. Although the term “thermoreversible gel” was originally introduced for polymer solutions,⁵ it is applied also to polymer melts, implying “reversible” nature of the interconnecting crystalline fibrils/stems under thermal influence.

The evolution of the dynamic moduli at early stages of crystallization was found to have the same universal pattern as chemical gelation.^{6–8} The physical gel point is manifested in slow power-law dynamics as expressed in the shear relaxation modulus

$$G(t) = St^{-n} \text{ for } \lambda_o < t < \lambda_{pg} \quad (1)$$

where S is the gel stiffness, n is the relaxation exponent, and λ_o is the crossover to short time dynamics (entanglements, segmental modes). The longest relaxation time of a physical gel, λ_{pg} , is finite in general; here, we find that the lifetime of the crystal structure is much longer than the experimental time and set $\lambda_{pg} = \infty$. However, stress relaxation experiments are lengthy and not applicable for fast solidification processes. Oscillatory shear is more informative and is favored in this study.

In oscillatory shear, the dynamic moduli at the gel point also follow power-law behavior

$$G'_c = \frac{G''_c}{\tan \delta} = S\Gamma(1-n)\cos \frac{n\pi}{2} \omega^n \quad \text{for } \omega < 1/\lambda_o, \quad (2)$$

that can be detected experimentally by a loss tangent, which becomes independent of frequency in the terminal zone

$$\tan \delta_c = \frac{G''_c}{G'_c} = \tan \frac{n\pi}{2} = \text{const} \quad \text{for } \omega < 1/\lambda_o. \quad (3)$$

SAOS needs to be performed in a low frequency window because power-law behavior of the dynamic moduli (eqs 2 and 3) is detected only in the terminal frequency zone.

Lack of molecular understanding of the physical origin of the arising connectivity initiated studies of structural properties of the growing clusters. Light scattering is a classical method for studying structure development during crystallization and phase separation processes.⁹ Although small-angle light scattering (SALS) experiments

have been reported for crystallizing polypropylene¹⁰ and polyethylene,¹¹ these studies were performed at high degrees of undercooling that resulted in fast crystallization kinetics, and made it difficult to monitor the initial stages near the gel point.

We focused our recent studies of polypropylene crystallization on the early stages at low undercooling (slow crystallization kinetics),^{12–14} that is, when molecular connectivity just arises and a network is beginning to be formed. In a combination of independent experiments, it is possible to measure the growth of crystallinity by DSC, the development of molecular connectivity by rheology, and the density and anisotropy fluctuations by SALS. This allows comparison of the time scales of crystallinity growth governed by Avrami time (DSC), connectivity growth governed by gel time (rheology), and evolution of cluster size governed by characteristic times of structure development (SALS). We found that the liquid–solid transition (gelation) occurs very early in the crystallization process. With increasing ΔT , the relaxation exponent n decreases from 0.8 to 0.5, gel stiffness S increases from 5,000 to 25,000 Pa s^{−n}. The gel time t_c at which the material passes through the gel point decreases exponentially.

Crystallinity growth (determined by DSC) followed a sigmoidal Avrami-type curve. The characteristic Avrami time is defined as the time at which the relative crystallinity reaches 63%. Crystallization kinetics may be described in terms of a dimensionless parameter, the ratio of gelation time to Avrami time t_c/t_A . This time ratio depends on the difference in the activation energy for the system to interconnect (gelation) or to crystallize (ordering). For iPP this ratio is very low $0.1 < t_c/t_A < 0.4$, that is, gelation (connectivity growth) occurs at the very early stages of the crystallization process.¹² The relative crystallinity of the critical gel of iPP, as determined by rheology/DSC, is about 2% or less. This observation raises basic questions about the underlying structure. How can it be that the growth rate of network formation is so much higher than the rate of bulk crystallization? What is the morphology of the sample spanning network structure?

Small-angle light scattering patterns of iPP (without shear) at the gel point show circular symmetry in both Hv and Vv modes and confirm the very low anisotropy of the growing clusters.¹³ The maximum in density fluctuation occurs very close to the rheologically obtained gel point. Orientation fluctuations develop much more slowly

and appear at much later stages of the crystallization process. This suggests that the critical gel state is characterized by strong density fluctuations. The average size of these density fluctuations (according to Debye–Bueche approach) is about 1 μm . High density fluctuations and low crystallinity of the critical gel reveal its heterogeneous, mostly amorphous microstructure. At late stages, SALS patterns display two-fold and four-fold symmetry in Vv and Hv modes, respectively, indicating the development of highly anisotropic structures. Optical microscopy indicates that these anisotropic structures at the late stages of crystallization are volume-filling spherulites.

Dynamic mechanical spectroscopy was used recently to follow the crystallization behavior of polyolefins.^{15, 16} The rise of the complex modulus has been correlated with the growth of crystallinity. The growth of G' has been attributed to the filler effects of the crystals, treating the system as a suspension. However, the crystallinity is extremely low at the gel point^{12–14} and early stages of crystallization cannot be explained in terms of suspension physics. However, the growth of G' can be used for estimating the gel point, as will be shown below.

Early stages of crystallization under shear were even less studied because of the complexity of the phenomena involved. However, it is realized that the rheology of undercooled melts strongly depends on the course of crystallization (and resultant morphology), which in turn is greatly determined by the history of deformation. This can explain the high sensitivity of processing to small changes in molecular details, which drastically affect crystallization and, hence, the connectivity and the stiffness of the gel as observed by rheology and processing. The understanding of morphology development during processing is at the heart of the optimization of synergy between polymer chain structure, processing, and final product performance. The problem may further be complicated by the complex nature of the type of flow in polymer processing. Pioneering studies of shear-induced crystallization of polypropylenes have been reported by the Linz school.^{17–19} Experiments were performed using inhomogeneous pipe flow with parabolic profile and high shear rates, while a narrow crystallization zone is moving from the cooled surface into the bulk of the polymer. The advancing crystallization zone in inhomogeneous flow was monitored during non-isothermal crystallization at different wall temperatures, and the shapes of the zones were cal-

culated. Crystallization kinetics and structural development were followed during nonisothermal and isothermal crystallization by monitoring the optical retardation, and increasing turbidity in time. These highly sensitive optical properties revealed early stages of crystallization—the kinetics of shear nucleation was studied and different modes of formation of the nuclei and their type were determined. Nucleation models are able to relate nucleation rate with shear rate and shearing time. Similar experiments have recently been performed by Kornfield and co-workers.²⁰

In this article, we report effects of shear strain on the early stages of crystallization, that is, on the physical properties of the critical gel, as studied by rheology. The goal was to study the effect of shear on the gel time. Early crystallization kinetics and rheological properties during strain-enhanced crystallization are compared with conventional quiescent crystallization.

EXPERIMENTAL

Materials

We studied a Ziegler–Natta isotactic polypropylene (iPP) homopolymer from Fina Co. (referred to as sample B in reference¹² and the same one characterized by SALS¹³). Molecular weights and polydispersity of the sample were measured using gel permeation chromatography (GPC) at Exxon Chemical, Baytown, Texas. The sample is of a high molecular weight and high polydispersity: $M_n = 84,200$ dalton, $M_w = 351,200$ dalton, $M_z = 1004,800$ dalton, $M_w/M_n = 4.2$, $M_z/M_w = 2.9$.

Rheological Experiment

Rheological experiments were performed with a Viscotech Rheometer from ATS Rheo Systems, Inc. (Sweden), equipped with cone/4° and plate (diameter 25 mm). Creep experiments with constant and high-stress level ($\tau = 12,000$ Pa) were followed by small amplitude oscillatory shear (SAOS) using the time resolved rheometry technique.²¹ Cone and plate geometry provides homogeneous flow (uniform strain) to the undercooled melt between the fixtures as compared to plate and plate geometry, which provide radially dependent strain. The sample was melted directly in the rheometer at 200 °C for 10 min under nitrogen, then was cooled to a crystallization tem-

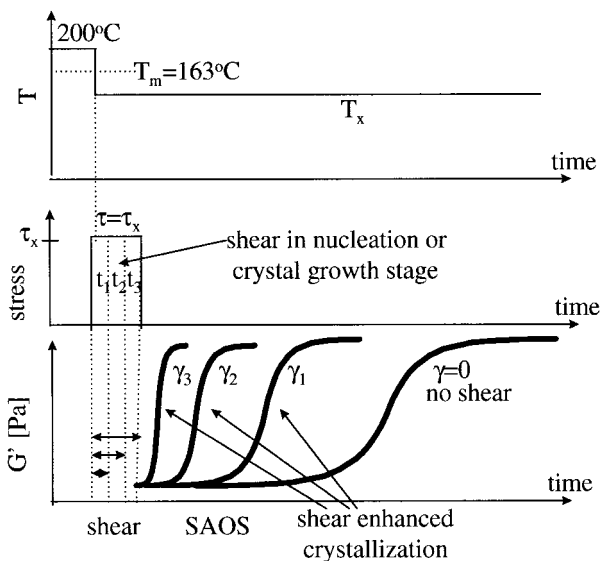


Figure 1. Schematics of temperature and shear protocol. Modulus growth for the undercooled melt during nucleation and crystal growth.

perature $T_x = 140$ °C, still in a nitrogen atmosphere, and held there for isothermal crystallization. The crystallization process was studied at frequencies $\omega = (0.04 - 5)$ rad/s.

Strain-enhanced crystallization was studied by first applying shear creep with a large strain (up to $\gamma = 300$) to the undercooled melt for a short time (from 5 s to 100 s) and then by SAOS at small strain amplitude ($\gamma = 0.01$) for gel-point detection. Shear creep was applied to the undercooled melt either during the nucleation stage (i.e., immediately after undercooling) or during crystallization (i.e., after annealing the undercooled melt at crystallization temperature $T_x = 140$ °C for 30 min until the sample was close to gel point). After deformation up to a prescribed strain, the flow was stopped and solidification behavior was monitored by SAOS (see Fig. 1). Sequential dynamic tests, that is, large strain followed by SAOS, have the advantage of quantitative gel-point detection from low frequency power-law behavior (eqs 2 and 3).

RESULTS AND DISCUSSION

Gelation after Strain in Nucleation and in Crystallization Stage

Gel times were determined following power-law behavior of the dynamic moduli in the terminal

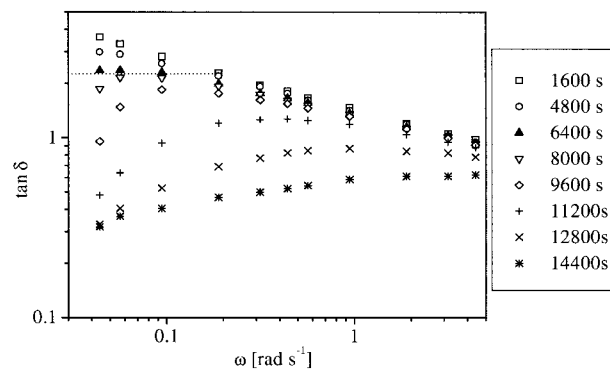


Figure 2. Tangent loss versus frequency at different instances during the crystallization process ($T_x = 140$ °C) after a strain of $\gamma = 0.1$ was applied in the nucleation stage. Different symbols depict crystallization times t_x . The estimated gel time is 6400s (▲).

zone.²² The gel point is detected by presenting the data in terms of the loss tangent and looking for the frequency independence of slow power-law dynamics. Figure 2 shows the plot of $\tan \delta$ versus frequency at different times. The “flat” phase angle region covers a low frequency window, as marked by a horizontal line. Using this method, we determined the gel times during isothermal crystallization of iPP with different histories of deformation (different strains). As expected, crystallization is strongly enhanced by the shear strain. Gel times decrease in a power law with increasing strain, see Figure 3. Strain applied at the crystal growth stage leads to a stronger decrease in gel time, that is, faster crystallization compared to strain applied at the nucleation stage.

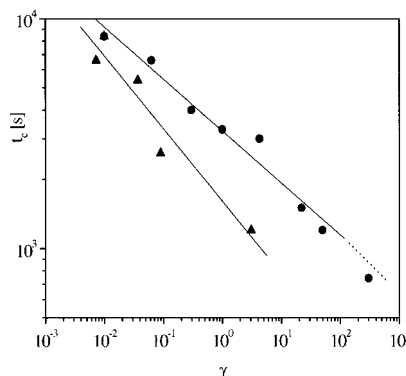


Figure 3. Gel times versus strain for isotactic polypropylene crystallized at $T_x = 140$ °C. Shear strain was applied at nucleation (circles) and crystallization (▲) stage. The gel time at highest strain $\gamma = 300$ (●) was determined by the proposed method.

Estimation of Gel Point for Rapid Gelation

The rate of crystallization increases with undercooling (large ΔT) and with imposed strain. This reduces the experimental time, which is available for mechanical spectroscopy²¹ and does not allow us to measure the power-law characteristics at the gel point. However, it is possible to measure the growth of the dynamic modulus at some constant experimental frequency. The experimental frequency needs to be chosen fairly high ($1 < \omega < 10$) rad/s in order to shorten the experimental time as much as possible. The question is whether the growth of the dynamic modulus will provide sufficient information for estimating the gel point. Initial results are presented in the following paragraphs.

With the increase of strain, the storage modulus growth curves shift to lower times and show more rapid evolution towards the solid state. The evolution of storage modulus at a single frequency of 5 rad/s for different strains is presented in Figure 4 [Fig. 4(a)—actual modulus data, Fig. 4(b)—normalized storage modulus]. Figure 4(a) shows that G'_{\min} is varying from $1 \cdot 10^4$ Pa to $2.5 \cdot 10^4$ Pa, which corresponds to variation in $\log G'_{\min}$ from 4.0 to 4.3, that is, 7.5%; G'_{\max} is varying from $1 \cdot 10^6$ Pa to $2 \cdot 10^6$ Pa, which corresponds to $\log G'_{\max}$ from 6.0 to 6.3, that is, 5%. Thus, the actual modulus grows by about 3 decades—experiments were carried out throughout the whole crystallization process from the typical melt behavior (liquid state), up to the torque limit of the rheometer (solid state). This gave possibility to probe rheologically different regimes of crystallization: nucleation, gelation, and gross crystallization. For further analysis in Figure 4(b), the storage modulus values were normalized by:

$$G'_{\text{norm}} = \frac{\log(G'(t)/G'_{\min})}{\log(G'_{\max}/G'_{\min})} \quad (4)$$

where G'_{\min} , $G'(t)$, and G'_{\max} are the storage moduli before crystallization, at intermediate times, and at the final stage of crystallization, respectively.

For slow crystallization, it is possible to study the growth of G'_{norm} and determine the instant of liquid-to-solid transition. Gel times for the low strains $0 \leq \gamma \leq 50$ were determined from power-law behavior according to the procedure shown in Figure 2, when $\tan \delta \neq f(\omega)$. We found that the gel time coincides with the instant when the normalized storage modulus had grown to values of

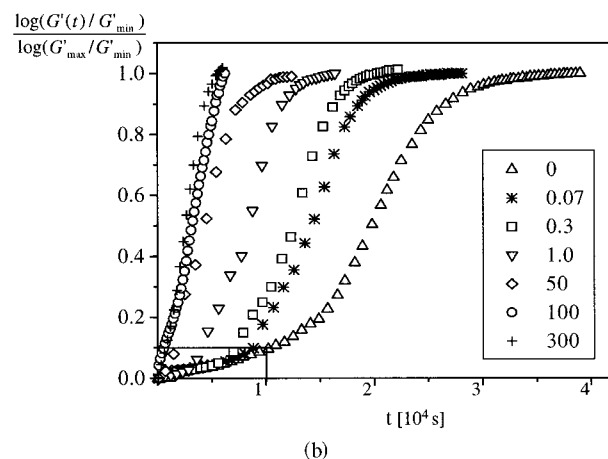
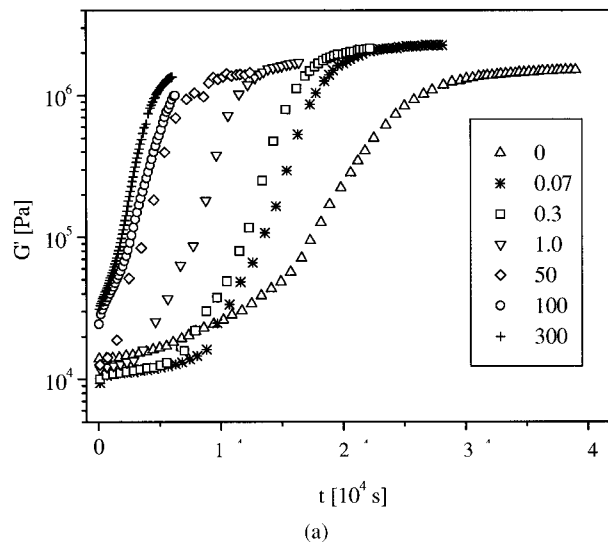


Figure 4. Actual storage modulus growth G' (a) and normalized modulus G'_{norm} (b) for isotactic polypropylene at single frequency $\omega = 5$ rad/s, strain amplitude of SAOS $\gamma_a = 0.01$ and $T_x = 140$ °C. The values in the label represent the shear strain γ applied in nucleation stage. For $0 \leq \gamma \leq 50$ data are subtracted from multifrequency sweeps, for $\gamma \geq 100$ data are taken only at a single frequency $\omega = 5$ rad/s.

about 0.05 to 0.10. The shape of $G'_{\text{norm}}(t)$ is nearly independent of frequency for our experiments. Based on these observations we propose an approximate method for detecting GP in rapidly crystallizing samples. For estimating the GP, we chose to use the time when the normalized storage modulus reached 10% of its maximum value.

The shape of the storage modulus growth curve characterizes the overall crystallization rate and reflects the type/history of applied deformation. Experimental curves at different strains (Fig. 4) are fitted with a Weibull type equation²³ (used

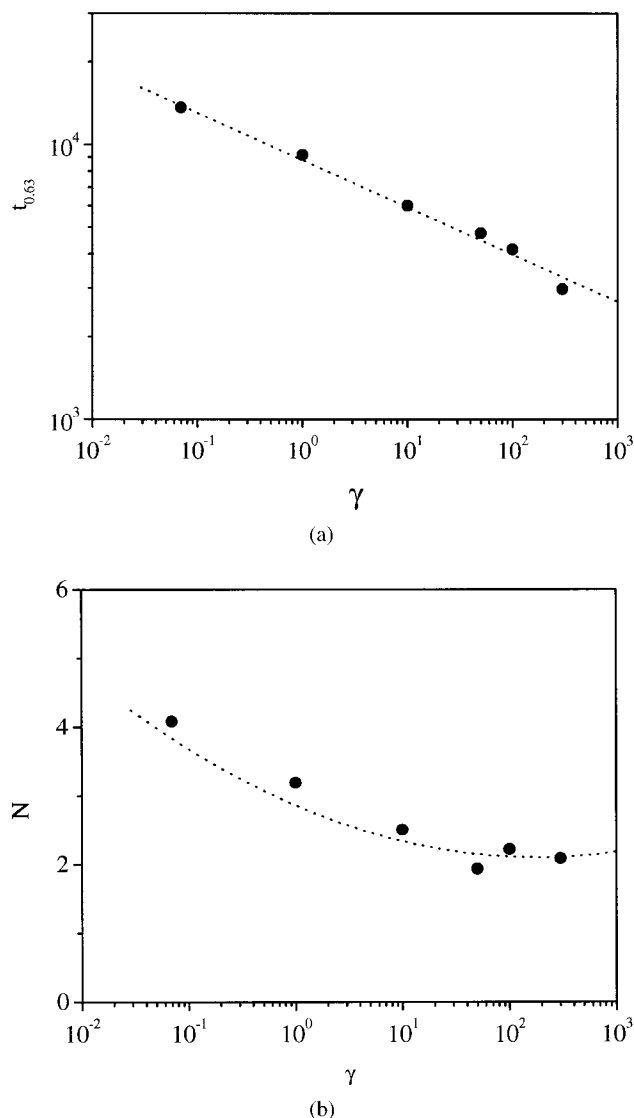


Figure 5. Empirical Weibull fit parameters for iPP at $T_x = 140$ °C (see eq 4): characteristic crystallization time (a) and exponent (b) versus applied strain.

also by Avrami²⁴) with two empirical parameters (characteristic modulus growth time $t_{0.63}$ and exponent N):

$$G'_{\text{norm}} = 1 - \exp(-(t/t_{0.63}(\gamma))^{N(\gamma)}) \quad (5)$$

$t_{0.63}$ denotes a reference state at late crystallization stages when, at $t = t_{0.63}$, the normalized modulus $G'_{\text{norm}} = 1 - 1/e$ adopts a value of 0.63 (any N). The applied strain on the iPP sample shifts the storage modulus growth curves to shorter times and, hence, decreases $t_{0.63}$ [Fig. 5(a)]. The

corresponding value of exponent N ranges between 2–4 [see Fig. 5(b)].

Storage Modulus Growth at High Strains

At very high strains ($\gamma > 100$), the storage modulus growth curves deviate from the single sigmoidal behavior—the modulus grows rapidly at short times, then slows down, and at later times, starts to grow rapidly again [Fig. 6(a)]. In other words, two successive exponents are necessary to represent kinetics after high strain. This results in a relative broadening of modulus growth

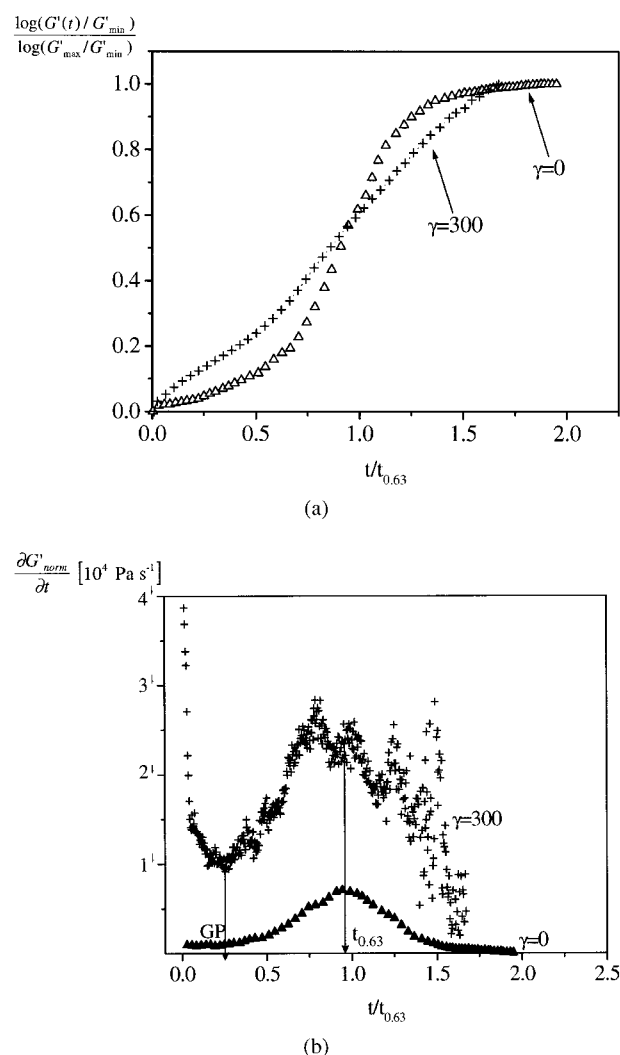


Figure 6. Normalized storage modulus growth G'_{norm} (a) and rate of storage modulus growth (dG'_{norm}/dt) (b) versus normalized time $t/t_{0.63}$ for isotactic polypropylene at $\gamma = 0$ (Δ) and at $\gamma = 300$ (crosses); $\omega = 5$ rad/s and $T_x = 140$ °C. Gel time and characteristic crystallization time are marked by the arrows; data of Figure 4.

curves. Broadening of G'_{norm} at high strains, which results in the decrease of N in Figure 5(b), becomes evident when a relative time scale is used [i.e., time scale is normalized to $t_{0.63}$, see Fig. 6(a)]. The growth curve at $\gamma = 300$ on Figure 6(a) shows two inflection points, which are more clearly seen on Figure 6(b), where the rate of storage modulus growth is plotted. The first inflection point occurs near the critical gel point and the second at later stages of solidification, near $t \approx t_{0.63}$. This indicates the complexity of the underlying mechanism of strain-induced crystallization and suggests at least two stages in the structure development under shear. At the first stage, crystalline strands are assumed to interconnect into a network, that is, loose, unstable crystals are formed. At the second stage intense crystallinity growth within the network proceeds, that is, hardening of the material occurs.

Generally speaking, large strain has the competing effects of network disruption on one side and accelerated crystallization (i.e., connectivity growth) on the other side. Which of those two processes prevails can be found by the behavior of storage modulus in time $G'(t)$. Increase of $G'(t)$ with time indicates a solidification (gelation) process, whereas its decrease may be interpreted as breaking of the material. The shear induced acceleration of the crystallization seems to be the overpowering process for the studied isotactic polypropylene, at least in the strain range applied.

CONCLUSION

Rheological studies demonstrate the strong acceleration of crystallization (and with it the obtained morphology) by shear. For preshearing at constant shear stress up to a prescribed strain level, gel times decrease in a power law with increasing strain. Strain applied during the crystallization stage accelerates gelation much more than strain applied in the nucleation stage.

An attempt is made to establish the relation between rheological behavior and crystallization by fitting Weibull-type functions to the growing storage modulus with two empirical parameters: characteristic time of modulus growth, $t_{0.63}$, and exponent N . This allows proposal of a method for gel point estimation for rapid gelation at intermediate strains, as long as the shape of the storage modulus growth curve shows single sigmoidal be-

havior. At very high strains, the storage modulus growth curves deviate from the single sigmoidal behavior, which precludes the use of this gel point estimation method. High strain experiments show the complexity of the underlying mechanisms of strain-induced crystallization, and reflect at least two possible stages in the structure development under shear. At the first stage, crystalline strands are interconnected into a loose network; and at the second stage, intense crystallinity growth within the network proceeds. Of course, the same two stages are obviously present during slow solidification at low strain or low undercooling. Experiments showed, however, that in rapid solidification (enhanced by strong thermal or dynamic force) each of these two sequential stages are enhanced individually.

Because of lack of structural data, we attribute the shear-enhanced crystallization to two different mechanisms. In the nucleation stage, shear might introduce additional nuclei or decrease the critical nucleus size, whereas shear during the crystal growth stage may preferably cause orientation and extension of clusters because of the applied strain. Stretched clusters growing in an undercooled melt might have a higher probability to interconnect (impinge) in comparison with nondeformed clusters. Formation of additional nuclei also proceeds when shear gets imposed in the crystallization stage.

The heterogeneous microstructure (large density fluctuation, low crystallinity) of the critical gel could depend strongly on small variations in molecular composition (stereoregularity, tacticity, molecular weight and MWD, nucleating agent, etc.), as well as on the deformation history. More studies are needed on the early stages of crystallization under strain to explore, on a quantitative level, the effect of the history/type of deformation on the rheological properties (stiffness, solidification rate) of the critical gel. In the future, flow effects on morphological characteristics of the critical gel will need to be considered to understand the molecular mechanisms that govern the gelation process. These studies have significant industrial importance in predicting/controlling structure development, the connectivity growth, and the stiffness of the gel during processing.

The authors acknowledge support under the MRSEC program at the University of Massachusetts at Amherst (NSF DMR 9809365) and from Exxon Chemical, Baytown, Texas.

REFERENCES AND NOTES

1. Mandelkern, L. *Crystallization of Polymers*; McGraw-Hill: New York, 1964; p. 359.
2. Fatou, J. G. *Crystallization Kinetics*. In *Encyclopedia of Polymer Science and Engineering*; Supplement. Wiley: New York, 1989.
3. *Crystallization of Polymers*; Dosiere, M., Ed.; Kluwer Academic Publishers: Norwell, MA, 1993. Printed in Netherlands.
4. Phillips, P. J. *Polymer Crystals*. *Rep Prog Phys* 1990, 53, 549–604.
5. Berghams, H.; Donkers, A.; Frenay, L.; Stoks, W.; De Schryver, F. E.; Moldenaers, P.; Mewis, J. *Polymer* 1987, 28, 97–102.
6. Winter, H. H.; Mours, M. M. *Adv Polym Sci* 1997, 134, 165–233.
7. te Nijenhuis, K.; Winter, H. H. *Macromolecules* 1989, 22, 411.
8. Lin, Y. G.; Mallin, D. T.; Chien, J. C. W.; Winter, H. H. *Macromolecules* 1991, 24, 850.
9. Stein, R. S.; Cronauer, J.; Zachmann, H. G. *J Mol Struct* 1996, 383, 19.
10. Okada, T.; Saito, H.; Inoue, T. *Macromolecules* 1992, 25, 1908.
11. Akpalu, Y.; Kielhorn, L.; Hsiao, B. S.; Stein, R. S.; Russell, T.P.; van Egmond, J. W.; Muthukumar, M. *Macromolecules* 1999, 32, 765–770.
12. Pogodina, N. V.; Winter, H. H. *Macromolecules* 1998, 31, 8164–8172.
13. Pogodina, N. V.; Siddiquee, S. K.; van Egmond, J. W.; Winter, H. H. *Macromolecules* 1999, 32, 1167–1174.
14. Schwittay, C.; Mours, M.; Winter, H. H. *Faraday Discuss* 1995, 101, 93.
15. Carrot, C.; Guillet, J.; Boutahar, K. *Rheol Acta* 1993, 32, 566–574.
16. Boutahar, K.; Carrot, C.; Guillet, J. *Macromolecules* 1998, 31, 1921.
17. Eder, G.; Janeschitz-Kriegl, H.; Liedauer, S. *Prog Polym Sci* 1990, 15, 629–714.
18. Liedauer, S.; Eder, G.; Janeschitz-Kriegl, H.; Jerschow, P.; Geymayer, W.; Ingolic, E. *International Polymer Processing* 1993, 8, 236–250.
19. Eder G.; Janeschitz-Kriegl, H. *Mater Sci Technol* 1997, 18, 269–342.
20. Kumaraswamy, G.; Verma, R. K.; Issaian, A. M.; Wang, P.; Kornfield, J. A.; Yeh, F.; Hsiao, B. S. *Abstracts of APS Meetings, Part II*, 44, N1, 1561, March 1999, Atlanta, GA.
21. Mours, M.; Winter, H. H. *Rheol Acta* 1994, 33, 385–397.
22. Holly, E. E.; Sundar, K.; Venkataraman, S.; Chambon, F.; Winter, H. H. *J Non-Newtonian Fluid Mech* 1988, 27, 17.
23. Weibull, W.; Sweden, S. *J Appl Mech* 1951, 9, 293–297.
24. Avrami, M.; *J Chem Phys* 1939, 7, 1103–1112; 1940, 8, 212–224; 1941, 9, 177–184.